JOURNAL OF CATALYSIS 93, 321–330 (1985)

Selected Area Fourier Transform Infrared Studies of Surface Reaction Dynamics

III. Spatial Coverage and Temperature Patterns during Self-sustained Oscillations of CO Oxidation on Pd/SiO_2

DAVID J. KAUL AND EDUARDO E. WOLF[1]

Department of Chemical Engineering, University of Notre Dame, Notre Dame, Indiana 46556

Received October 3, 1984; revised January 8, 1985

Surface dynamics of self-sustained oscillations during CO oxidation on a 2 wt% Pd/SiO_2 catalyst have been studied using Selected Area Fourier Transform Infrared (FTIR) spectroscopy along with temperature measurements from an array of four sensitive surface thermocouples. These experiments demonstrate that self-sustained oscillations involve spatially propagating regions of nonuniform coverage and surface temperature. The results elucidate how the multipeak structure of the oscillations arises from inhomogeneous patterns in surface reaction rate controlled by localized CO inhibition.

INTRODUCTION

During recent years, numerous reports have been published documenting the observation of self-sustained oscillations during catalytic reactions and several extensive review articles are available (*1–6*). An equal number of theoretical models have been proposed to simulate such oscillations (*7–17*). Our previous transient Fourier Transform Infrared (FTIR) studies during CO oxidation on a 5 wt% Pt/SiO_2 catalyst (*18*) have demonstrated a complex dynamic behavior of surface temperature and surface coverage not previously reported. By using four sensitive foil thermocouples touching four equidistant points on the surface of a catalyst wafer, we have clearly shown the occurrence of spatially nonuniform temperatures during oscillatory behavior (*19*). In contrast to the localized nature of these temperature measurements, it was emphasized that the FTIR measurements were obtained over a catalyst area of 2.5 cm^2 and therefore represented an area average value which might conceal a spatial distribution in the coverage of adsorbed CO. The lack of correlation between the local surface temperatures and the area averaged CO coverage led us to the realization that similar spatial nonuniformities should be present for adsorbed CO. The results presented in this paper using Selected Area FTIR measurements confirm for the first time that such spatial nonuniformities in CO coverage occur during oscillatory behavior on a supported catalyst. Furthermore, the dynamic behavior of local CO coverage correlates well with the localized temperatures and indicates further that propagating waves of temperature and CO coverage occur during oscillatory behavior. These observations are reported for a 2% Pd/SiO_2 catalyst which exhibits the same type of thermokinetic oscillations as the Pt/SiO_2 system.

EXPERIMENTAL

Apparatus and procedure. Details of the experimental apparatus and procedure have been presented previously (*18, 19*), consequently only a brief summary of the main features relevant to this work will be presented here. The computerized FTIR spectrometer (Digilab FTS-15C) is capable of rapid data acquisition and storage of

[1] To whom correspondence should be addressed.

0021-9517/85 $3.00

thousands of complete mid-IR spectra during a typical 2-h experiment. Subsequent computer analysis yields an infrared "spectragram" which displays the baseline corrected absorbance peak height as a function of time at the preselected frequencies of adsorbed species. A small-volume (6 cm^3) IR cell reactor is fitted with CaF_2 windows in a design that permits a high-temperature operation (>400°C) without the need of special cooling. Four gas flow ports allow a dual inlet–outlet operation with either cocurrent or countercurrent flow past the catalyst wafer. Programmable flow and temperature controllers permit concentration or temperature-programmed reaction studies (CPR or TPR) to be carried out at any desired programming rate and within any desired range of temperature and concentration. Four delicate foil thermocouples which have a millisecond response time provide a unique, sensitive measurement of what we consider the local catalyst surface temperature. The four thermocouples are arranged so that they sample both sides of a 1-cm square region located at the center of the 2-cm-diameter catalyst wafer. The thermocouples located diagonally opposite each other are on the same side of the wafer as depicted in Figs. 2–4 along with the countercurrent mode of operation used for these experiments. The thermocouple arrangement allows determination of temperature variation in the axial direction, as well as directions perpendicular to flow.

Selected Area FTIR measurements. A unique new feature of our system provides for selective determination of coverage variation in the axial and radial direction. This was accomplished by fitting a rotatable aperture to the reactor window in the path of the incident IR beam. This selected area aperture exposed only one of four quadrants of a circle having the same diameter as the catalyst and could be rotated to any one of four preset positions. Each position was such that one of the four thermocouples sampled the center of the irradiated quadrant and the total of the four regions sampled the entire surface area of the catalyst wafer. This spatial arrangement is depicted in Figs. 2–4. Self-sustained oscillations were studied by collecting data for one hour from each region sequentially.

During IR analysis of one quadrant, the information from the other three cannot be simultaneously acquired and it is necessary to repeat the analysis for each quadrant, starting at the same point in the oscillatory wave. Thus the superimposed behavior of the four quadrants is representative of the oscillatory period only if the oscillations are periodic. Oscillations observed on a 2% Pd/SiO_2 catalyst have shown remarkable periodicity, consequently they are specially suited to be studied by the selected area FTIR technique.

Catalyst. The 2% Pd/SiO_2 catalyst used in this study was prepared by the wet impregnation technique. The support was a commercial high surface area SiO_2 (588 m^2/g, Harshaw). A 200-ml solution of methylene chloride containing the required amount of Pd(II) acetylacetonate was equilibrated under constant stirring with 10 g of support for 16 h at room temperature. The solvent was then evaporated by heating at 40°C for 2 h with continuous stirring. After the catalyst was dried in air overnight at 100°C, it was pretreated in flowing oxygen (100 cm^3/min) for 4 h at 250°C and 2 h at 400°C to ensure complete decomposition of Pd acetylacetonate and subsequent oxidation to Pd^{2+}. The calcined catalyst was flushed with Ar for 1 h while cooling the reactor to 250°C and then reduced in flowing 20% H_2/Ar (100 cm^3/min) for 4 h at 250°C and another 2 h at 400°C. TEM measurements indicate an average crystallite size of 100 Å. A catalyst disk, 2 cm in diameter and 0.1 mm thick, was pressed from 0.03 g of the powder under a pressure of 10,000 psi. The resultant self-supporting wafer had a BET surface area of 515 m^2/g, whereas the powder form of the catalyst had 590 m^2/g of surface area.

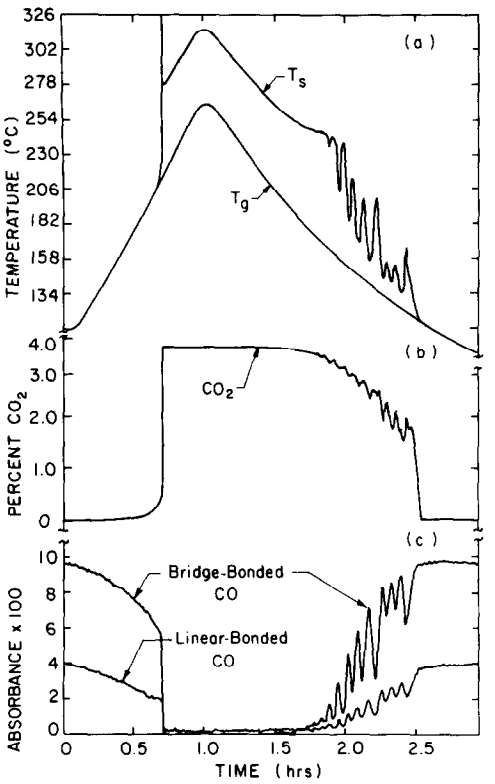

FIG. 1. TPR experiment with gas mixture of 9.0 cm^3/min CO, 5.0 cm^3/min O_2, and 200 cm^3/min N_2. (a) Programmed reactor temperature curve and response of surface temperature. (b) Response of CO_2 production. (c) Spectragram for linear- and bridge-bonded forms of CO on Pd.

RESULTS

Conditions that would give rise to kinetic oscillations were established using the temperature-programmed reaction (TPR) and concentration-programmed reaction (CPR) techniques described previously (*18, 19*). Once the oscillations were established, they could be sustained for as long as desired. Their initial oscillatory patterns generally evolved toward longer periods and greater amplitudes for up to 2 days before becoming invariant. The periods range from 6 to 15 min for temperatures between 90 and 150°C.

Figure 1 displays results of a TPR experiment showing: (a) reactor (T_g) and catalyst temperature (T_s); (b) CO_2 production, and (c) spectragrams of the CO adsorbed species. These results were obtained in our earlier reactor designed for a single inlet single outlet flow scheme described in detail elsewhere (*18*). The gas flow rates were held constant at 200, 9.0, and 5.0 cm^3/min for N_2, CO, and O_2, respectively, while the temperature was programmed to increase from 110 to 265°C and then decrease again to 110°C over a 3-h period. The catalyst temperature (T_s) reported in this figure corresponds to measurements obtained with a single foil thermocouple in contact with the wafer near the reactor inlet, whereas the reactor temperature, T_g, corresponds to a measurement obtained with a minithermocouple (Omega) positioned flush with the reactor wall. The later thermocouple signal also provided feedback to the temperature programmer.

The FTIR data was obtained by collecting 10,000 spectra in 1000 sets of 10 coadded scans. The IR results are displayed as a spectragram in Fig. 1 which shows the baseline corrected absorbance peak height as a function of time for the bridge-bonded CO species at 1980 cm^{-1} as well as the linear-bonded CO species at 2090 cm^{-1}. The assignments of these bands for CO on Pd have been reported previously (*20, 21*) as well as the predominance of the bridged forms as is shown in Fig. 1. The IR data in Fig. 1 was collected with the beam transmitted through the entire surface area of the catalyst wafer and thus it does not contain information on spatial distributions of CO coverage. We estimate that the quantitative detectability limit for these IR measurements corresponds to CO coverage of about 0.05 monolayer, based on comparison with the absorbance values obtained on a Pt catalyst wafer of equal thickness but 2.5 times the loading.

The features of Fig. 1 show the same type of ignition and quenching due to CO inhibition behavior previously reported for Pt/SiO_2 (*18, 19*). As the reactor temperature increases linearly, the reaction is ignited

from 14% to a high steady state yielding 92% conversion. Concurrently with this ignition, a rapid catalyst temperature excursion of about 110°C is observed, thereafter T_s follows T_g, but it remains at least 50°C higher throughout the region of high conversion. The absorbance of both bridged- and linear-bonded CO, initially high at low temperatures where the rate is inhibited by CO adsorption, decreases drastically as ignition occurs. After ignition, the linearly increasing temperature has no effect on CO_2 production. Past its preset maximum, T_g decreased linearly followed by a similar decrease in T_s, until the latter lags behind the reactor cooling rate, in fact increasing slightly, before entering an unstable oscillatory region at about 165°C. CO_2 production, which remained constant after ignition, began to decrease and oscillate in the unstable region until at 115°C, the reaction quenched completely.

As the reactor temperature decreases, CO coverage begins to increase and starts oscillating throughout the unstable region between 165 and 115°C. Clearly, both linear- and bridge-bonded CO oscillate in phase. The large fluctuations in CO coverage show an inverse but not proportional correlation with the small fluctuations in CO_2 production. Also in this region, the local catalyst temperature measurement shows excursions which are much larger than would be expected for the corresponding fluctuations in CO_2 production.

Reproducible self-sustained oscillations can be observed by bringing the reactor to the unstable region via TPR (or CPR) experiments, at which point the programming rate is halted and the reactor is operated with all inputs at steady state. A variety of oscillatory patterns can be reproducibly obtained in this way, depending on the CO/O_2 ratio and the reactor temperature. Generally, a decrease in the CO/O_2 ratio decreases the reactor temperature at which oscillations occur, and results in oscillatory patterns of larger amplitude. The experiments reported in Figs. 2–4 were obtained at a reactor temperature of 98°C and with $CO/O_2 = \frac{1}{3}$ ($N_2 = 180$, $CO = 9.0$, $O_2 = 27.0$ cm^3/min). These studies were carried out in a reactor equipped with an array of four surface thermocouples, using the countercurrent gas flow scheme described under Experimental. Figure 2 shows self-sustained oscillations in which the IR data was collected over the entire area of the wafer, whereas Figs. 3 and 4 show the selected area FTIR measurements for the same oscillatory state.

The oscillations obtained under the above conditions are shown for an elapsed time of 1 h in Fig. 2. The CO_2 production (Fig. 2a), IR spectragrams (Fig. 2b), and data from the four thermocouples (Figs. 2c to f) indicate that the oscillations are reproducible for as long as one chooses to observe them and have a fairly periodic cycle lasting about 10 min. Figure 2 also depicts schematically the thermocouples in their positions on the catalyst wafer and in their relationship to the countercurrent flow of the gases. The filled circles in the figure are on the same side as the gas flow indicated by the solid arrow, whereas the open circles and broken arrow correspond to the opposite side of the wafer.

Figures 2a and b show the structure of the oscillatory patterns obtained during 1 h. For simplicity, one cycle has been singled out in a darkened area to show the temperature and coverage correlations within the cycle. A similar cycle has been selected in Figs. 3 and 4. A cycle generally consists of two small peaks preceding a large one followed by one intermediate size satellite peak. Sometimes one or both of the small peaks are skipped but the major peak and its satellite occur in every cycle. The integral average value of CO_2 production can be seen to correlate inversely with the average coverage of adsorbed CO. Close inspection of the temperature oscillations traced by the four thermocouples reveals a spatial structure in the dynamic behavior. In order to describe this behavior, we have adopted a system of subscripts which indicates the

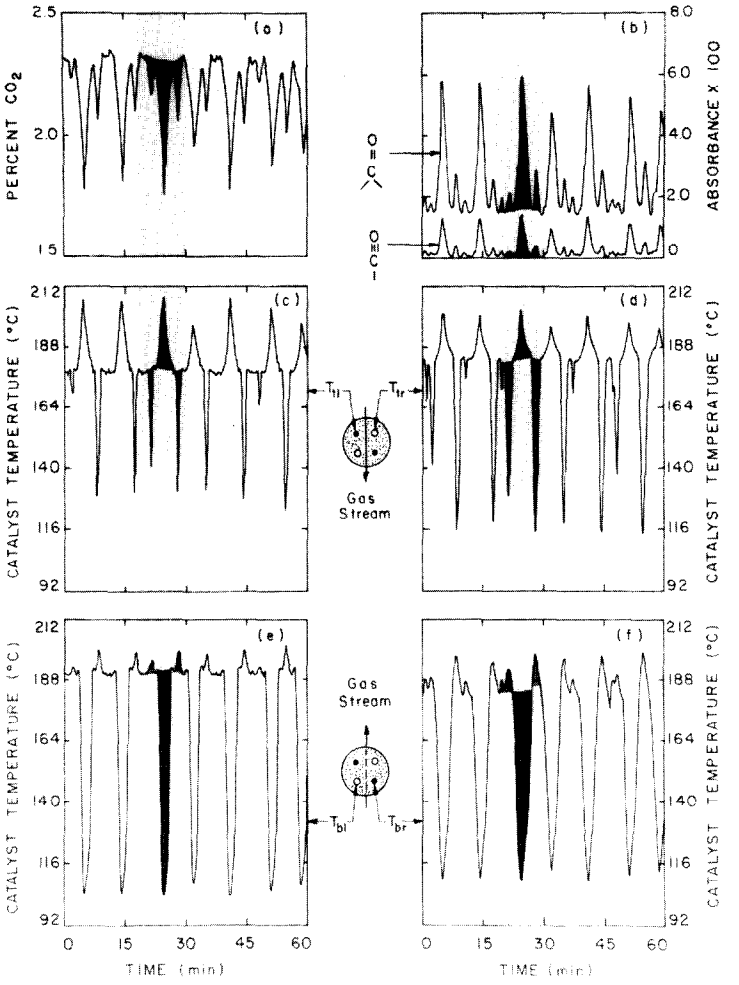

FIG. 2. Self-sustained oscillations obtained with 9.0 cm^3/min CO, 27.0 cm^3/min O_2, and 180 cm^3/min N_2 at 98°C. (a) Oscillations of CO_2 production. (b) Spectragram of adsorbed CO oscillations. (c–f) Surface temperature oscillations from an array of four thermocouples.

position of each thermocouple in the schematic relative to the viewers eye (i.e., top (t), bottom (b), left (l), or right (r)).

Thermocouples T_{tl} and T_{tr} located in the upper half of the wafer but at different sides, oscillate in phase. Likewise thermocouples T_{bl} and T_{br} located in the lower half of the wafer are also in phase with each other but completely out of phase with those in the upper half. This demonstrates that there is good synchronized thermal communication across the wafer and in the direction perpendicular to flow but a complete asynchronization along the direction axial to gas flow. In fact as the temperature in the upper half (T_{tl} and T_{tr}) reaches its maximum of about 205°C, it reaches a minimum at about 105°C in the lower half. The large dip in CO_2 production correlates with the sudden temperature drop in the lower half of the wafer but it certainly does not explain the simultaneous temperature increase in the upper half. Conversely, as the upper temperatures decrease, and pass through a minimum corresponding to one of the small peaks in CO_2 production, the tem-

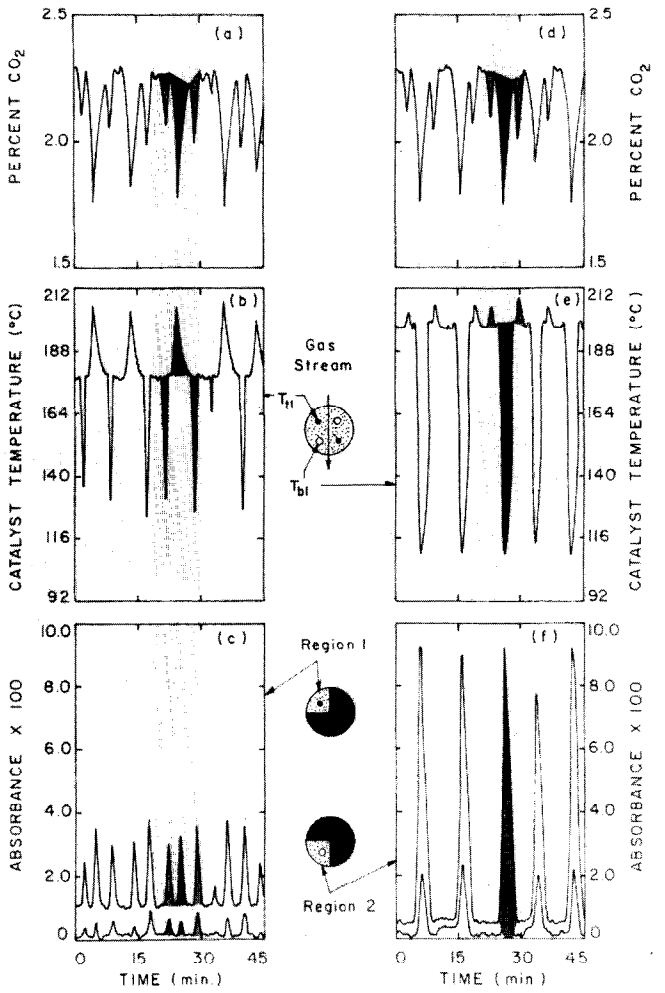

FIG. 3. Self-sustained oscillations studied by Selected Area FTIR. (a–c) Average CO_2 production and local surface temperature and selected area spectragrams of CO coverages for the top left quadrant. (d–f) Average CO_2, local surface temperature and selected area CO coverage results for the bottom left quadrant.

peratures in the lower half increase and pass through a maximum. These data seem to demonstrate that as a partial quenching occurs in the lower half, the upper section of the wafer is ignited to an abnormally high reaction rate and vice versa. This behavior clearly demonstrates the nonuniform spatial nature of the temperature distribution during these oscillations and the difficulty in attempting to match localized temperature values with the area average CO coverage and CO_2 production values.

In order to verify if the nonuniformities in temperature were related to nonuniformities in coverage, a quadrant of the wafer was selected for IR analysis using the selected area aperture method described under Experimental. Of course, it is not possible to record data from the four quadrants simultaneously, but due to the periodic nature of the oscillations the data recorded sequentially from different quadrants provides equivalent information.

Figure 3 shows the data taken sequen-

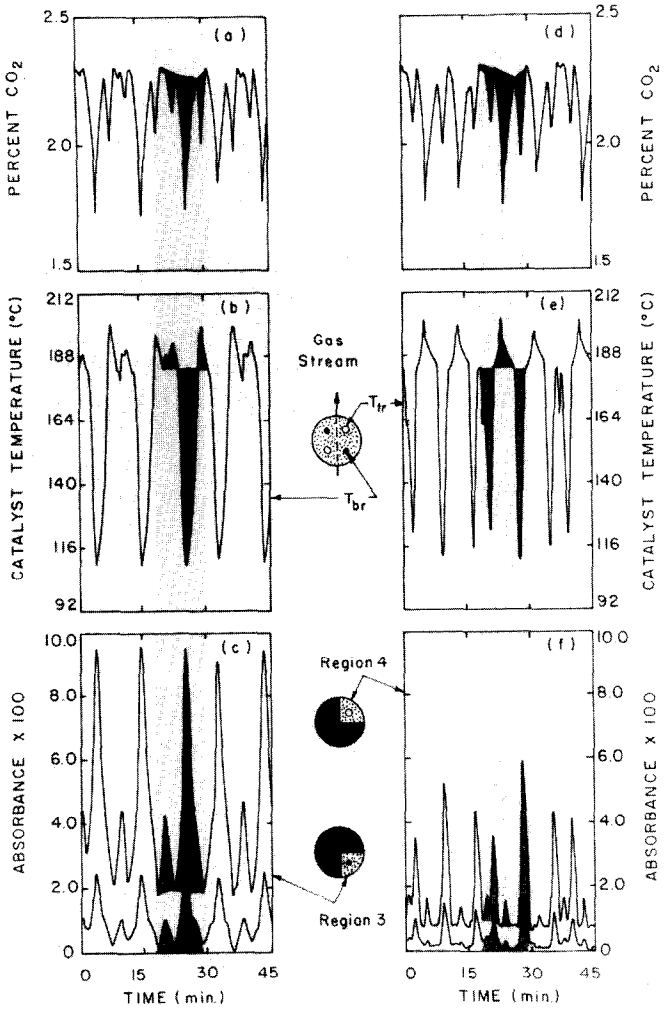

FIG. 4. Self-sustained oscillations studied by Selected Area FTIR. (a–c) Average CO_2 production and local surface temperature and selected area spectragrams of CO coverages for the top right quadrant. (d–f) Average CO_2, local surface temperature and selected area CO coverage results for the bottom right quadrant.

tially displaying CO_2 production, catalyst temperature and the IR spectragram corresponding to the left upper and lower quadrants. The temperature behavior and CO_2 production is as described in Fig. 2, however the IR information from the upper and lower quadrants are markedly different, showing for the first time that nonuniformities in CO coverage also occur. The brief and sharp temperature decrease in T_{tl} in the upper left quadrant (3b) correlates with a moderate increase in CO coverage in that quadrant (3c) and leads to the small decrease in CO_2 production (3a) preceding the major peak. During the corresponding portion of the CO_2 production cycle in the lower left quadrant (Figs. 3d–f), the CO coverage remains at a minimum and the catalyst temperature (T_{bl}) increases slightly. There is an excellent correlation between an increase in adsorbed CO in the bottom left quadrant and the large decrease in temperature (T_{bl}) and CO_2 production corresponding to the major peak. A second peak

in adsorbed CO in the upper left quadrant correlates with the major CO_2 production decrease, but occurs when T_{tl} is increasing through its maximum. This wrong-way temperature behavior appears to be the result of the quenching in the bottom half which extends partially into the upper quadrant but not as far in as the position of T_{tl}, leaving T_{tl}, within a region of abnormally high reaction rate. The intermediate size satellite peak following the major one duplicates the same coverage and temperature behavior described for the small peak preceding the major peak.

Figure 4 shows the behavior of the right top and bottom quadrants of the wafer. They basically duplicate, although not exactly, the behavior of the left side. Spatial nonuniformity in coverage occurs between the upper and lower right quadrants. Increases in coverage correlating with decreases in CO_2 production and in temperature in the top quadrant, while low coverage and higher than normal temperatures predominate in the bottom quadrant. The CO coverage on the right side contains an additional peak, mostly in the lower right quadrant, which gives rise to the fourth and barely discernible decrease in CO_2 production that follows the intermediate size satellite to the major peak.

A further demonstration of the local distribution of coverage can be realized when the individual values of upper and lower quadrants are compared with the area average value measured by the full beam (Fig. 2b). Clearly, the average value can be seen as resulting from the overlap of events occurring in each quadrant. The superimposed results from the full-beam measurement show a complicated four-peak cycle in surface coverage, however, the selected area FTIR measurements clearly show that the multipeak structure of these oscillations arises from spatial nonuniformities in the surface reaction rate. These results demonstrate how spatial nonuniformities can confuse the interpretation of surface measurements that yield an average value from a comparatively large area.

DISCUSSION

The following novel results have been obtained regarding CO coverage and surface temperature during dynamic behavior of CO oxidation on Pd/SiO_2:

(1) Oscillations in CO_2 production involve severely nonuniform spatial distributions in CO coverage and surface temperature.

(2) Spatial variations in CO coverage and temperature are minor in the directions perpendicular to the gas flow, but they are significant in the direction of the gas flow along the catalyst wafer (axial direction).

(3) The multipeak oscillatory pattern appears to be determined by the fluctuations of regions of the wafer at high and low steady state. The spreading of a region of high CO coverage, lower temperature, and inhibited CO_2 production in one region is partially counterbalanced by the occurrence of higher than normal reaction rates in another region operating at low CO coverage, high temperature, and high CO_2 production.

(4) The period of the oscillations is related to the rate at which propagating regions of high CO coverage spread out or recede along the catalyst surface in a wave-like motion.

These results experimentally confirm for the first time that reaction rate oscillations in a supported catalyst can involve propagation of regions of high surface concentration of adsorbed species. These Selected Area FTIR measurements, although not of high spatial resolution, clarify the existence of a spatial nature to the oscillations which could not be discerned from the normal IR measurements taken over a comparatively large area. In particular it clarifies our previous data (*19*) of oscillations on supported Pt which showed a local temperature increase with decreasing CO_2 production, and increasing CO coverages.

The studies reported here confirm that CO oxidation on supported Pd, like on Pt, exhibits the ignition, inhibition, and quenching phenomena characteristic of a

bimolecular Langmuir–Hinshelwood behavior in agreement with most recent studies on Pd single crystals (*22–24*). In the low steady state, the kinetic behavior is controlled by site blocking caused by high CO coverage which inhibits oxygen chemisorption and dissociation. In the high steady state, CO adsorption limited kinetics controls the reaction rate. Transition between low and high steady state is autocatalyzed by the heat of reaction and thus occurs instantaneously. Quenching from the high to low steady state, during TPR experiments, does not occur abruptly but as a series of oscillatory states which eventually die out as the reaction quenches. The behavior in the transition region is characterized by spatial nonuniformities in surface variables controlled by localized CO inhibition, whereas the high steady state is spatially uniform and has very low CO coverage.

Self-sustained oscillations are observed in this unstable region and initiate when a wave of high CO coverage is triggered to spread toward the catalyst center from one of the axial edges of the wafer. This advancing CO wave inhibits the reaction in much of the catalyst but leads to higher local turnover numbers at the crystallites within the restricted region of high steady state due to the local availability of more reactants. Thus a hot spot forms in a region of low coverage at the opposite edge from the advancing CO coverage wave. This region of high reactivity and temperature can then spread out from the opposite direction reigniting the quenched region and so on, in what appears as waves of high and low coverage moving back and forth along the wafer. The axial movement of these waves suggests that the gas flow over the catalyst synchronizes the behavior at the crystallite level. Clearly, the spatial propagation of these regions is not limited by diffusional or thermal transport since the time constants of these processes are much smaller than the periods of the oscillations. Furthermore, communication in the direction perpendicular to flow is adequate to maintain quasi-uniform conditions of temperature and coverage in that direction.

Experiments at different flow rates and flow directions result in different oscillatory patterns (amplitude, period) and alter somewhat the temperature and concentration window for the unstable region. More recent results indicate that even under conditions of high recycle, an axially propagating spatial structure still occurs during the oscillations. This indicates that the flow pattern, although important in determining the type of oscillation obtained, is not the condition causing oscillations. Since oscillations have been documented in unsupported forms of both Pt and Pd (e.g., foils, wire and single crystals) (*25–27*), and since radial nonuniformities are not observed in our wafer, it follows that nonuniformities in the preparation of the catalyst wafer are not the necessary condition for oscillatory behavior.

While this work shows experimentally for the first time the spatial nature of oscillations in a supported catalyst, it does not clarify the nature of the trigger mechanism that initiates the advance and controls the propagation of the CO wave. The recent ongoing work of Ertl and co-workers (*27–29*) has uncovered that self-sustained oscillations of CO oxidation on a Pt(100) single crystal are related to reversible surface phase transformations driven by changes in CO coverage. In a forthcoming paper (*30*), these authors provide evidence via dynamic LEED, of a wave-like propagation of alternating bands of two structural modifications of the Pt surface, one of which correlates directly with high CO coverage. Although no comparable dynamic LEED studies of oscillations on Pd have been reported, similar ordered structures and surface transformation on the Pd(100) surface have been documented in the past (*31, 32*) during steady-state LEED measurements. If such phase transformations, triggered by changes in CO coverage, can occur on foils, wires, and supported crystallites and lead to a change in reactivity of the surface, then this could indeed be the elusive mechanism

that underlies the observed oscillatory behavior on these catalysts. While the complex supported catalyst containing small crystallites and operating at atmospheric pressure used in our work, is clearly different from the Pt single crystal operating under high-vacuum conditions used by Ertl (*30*), the analogies between the two sets of results suggest that a connection may exist between the propagating phase transformations and our propagating CO waves.

The results reported in this work clearly demonstrate a role of inhomogeneous patterns in coverage and temperature during oscillatory states. We anticipate that this phenomena can play a role whenever dynamic conditions arise in exothermic catalytic reactions exhibiting multiplicity due to inhibition by an adsorbed species. The use of Selected Area FTIR measurements in this work clearly elucidates how the multipeak structure of oscillations can arise from spatially nonuniform reaction rates. While recent theoretical studies have explored the role of spatial inhomogeneities and pattern formation with regard to oscillatory states (*33, 34*), none incorporates the full range of phenomena reported here. It appears that the key to modeling oscillatory behavior occurs at the crystallite level and that future efforts will require models that are sufficiently general to account for competitive adsorption and surface reaction inhibition, along with a mechanism accounting for spatially nonuniform states.

ACKNOWLEDGMENTS

Funds for the FTIR Spectrometer–reactor system were provided by NSF Equipment Grant ENG 79-11459.

REFERENCES

1. Sheintuch, M., and Schmitz, R. A., *Catal. Rev.-Sci. Eng.* **15**(1), 107–172 (1977).
2. Slinko, M., and Slinko, M., *Catal. Rev.-Sci. Eng.* **17**(1), 119 (1978).
3. Bykov, V., and Yablonskii, C., *Int. Chem. Eng.* **21,** 59 (1981).
4. Hlavacek, V., and Vortruba, J., "Advances in Catalysis," Vol. 27, p. 59. Academic Press, New York, 1978.
5. Eigenberger, G., *Chem.-Ing.-Tech.* **50**(12), 924 (1981).
6. Hlavacek, V., and van Rompay, P. V., *Chem. Eng. Sci.* **36,** 1587 (1981).
7. Hugo, P., and Jakubith, M., *Chem.-Ing.-Tech.*, **44,** 383 (1972).
8. Dagonnier, R., and Nuyts, J., *J. Chem. Phys.* **65,** 2061 (1976).
9. Lagos, R. E., Sales, B. C., and Suhl, H., *Surf. Sci.* **82,** 525 (1979).
10. Vayenas, C. G., Lee, B., and Michaels, J., *J. Catal.* **66,** 36 (1980).
11. Sales, B. C., Turner, J. E., and Maple, M. B., *Surf. Sci.* **114,** 381 (1982).
12. Pikios, C. A., and Luss, D., *Chem. Eng. Sci.* **32,** 191 (1977).
13. Jensen, K. F., and Ray, W. H., *Chem. Eng. Sci.* **35,** 2439 (1980).
14. Jensen, K. F. and Ray, W. H., *Chem. Eng. Sci.* **37,** 1387 (1982).
15. Berman, A. D., and Krylov, O. V., *Int. Chem. Eng.* **20**(2), 313 (1980).
16. Reikert, L., *Ber. Bunsenges. Phys. Chem.* **85,** 297 (1981).
17. Dagonnier, R., Dumont, M., and Nuyts, J., *J. Catal.* **66,** 130 (1980).
18. Kaul, D. J., and Wolf, E. E., *J. Catal.* **89,** 348 (1984).
19. Kaul, D. J., and Wolf, E. E., *J. Catal.* **91,** 216 (1985).
20. Eischens, R. P., Francis, S. A., and Pliskin, W. A., *J. Phys. Chem.* **60,** 194 (1956).
21. Baddour, R. F., Modell, M., and Goldsmith, R. L., *J. Phys. Chem.* **74,** 1787 (1970).
22. Conrad, H., Ertl, G., and Kuppers, J., *Surf. Sci.* **76,** 323 (1978).
23. Engel, T., and Ertl, G., *J. Chem. Phys.* **69,** 1267 (1978).
24. Matsushima, T., *J. Catal.* **64,** 38 (1980).
25. Schmitz, R. A., and Plichta, R. T., *Chem. Eng. Commun.* **3,** 387 (1979).
26. Turner, J. E., Sales, B. C., and Maple, M. B., *Surf. Sci.* **103,** 54 (1981).
27. Ertl, G., Norton, P. R., and Rustig, J., *Phys. Rev. Lett.* **49,** 177 (1982).
28. Thiel, P. A., Behn, R. J., Norton, P. R., and Ertl, G., *Surf. Sci.* **121,** L553 (1982).
29. Cox, M. P., Ertl, G., Imbihl, R., and Rustig, J., *Surf. Sci.* **134,** L517 (1983).
30. Cox, M. P., Ertl, G., and Imbihl, R., submitted for publication.
31. Matters, A. M., Goodman, R. M., and Somorjai, G. A., *Surf. Sci.* **7,** 26 (1967).
32. Janko, A., Polczewska, W., and Szymorska, I., *J. Catal.* **61,** 264 (1980).
33. Sheintuch, M., and Pismen, L. M., *Chem. Eng. Sci.* **36,** 489 (1981).
34. Jensen, K., *Chem. Eng. Sci.* **38,** 855 (1983).